L-Diffusion: Laplace Diffusion for Efficient Pathology Image Segmentation

Weihan Li [1 2] Linyun Zhou [1 2] Jian Yang [1 2] Shengxuming Zhang [1 2] Xiangtong Du [3]
Xiuming Zhang[* 4] Jing Zhang [4] Chaoqing Xu[* 5] Mingli Song [1 2 6] Zunlei Feng[* 1 2 6]

1 State Key Laboratory of Blockchain and Data Security, Zhejiang University

2 School of Software Technology, Zhejiang University

3 School of Medical Imaging, Xuzhou Medical University

4The First Affiliated Hospital, College of Medicine, Zhejiang University

5 School of Computer and Computing Science, Hangzhou City University

6 Hangzhou High-Tech Zone (Binjiang) Institute of Blockchain and Data Security

code

Diffusion for Segmentation

■ Why diffusion is suitable for segmentation

- ➢ Shape Structure Emerges through Reverse Diffusion ➔Acting on **Feature Space** **(Intermediate convolutional features)**
- ➢ Semantic Boundaries Form without Explicit Supervision➔Acting on **Image Space** **(Pixel-level edge)**
- ➢ Noise-Induced Diversity Enhances Category Separation ➔Acting on **Latent Space** **(Latent after encoder compression)**

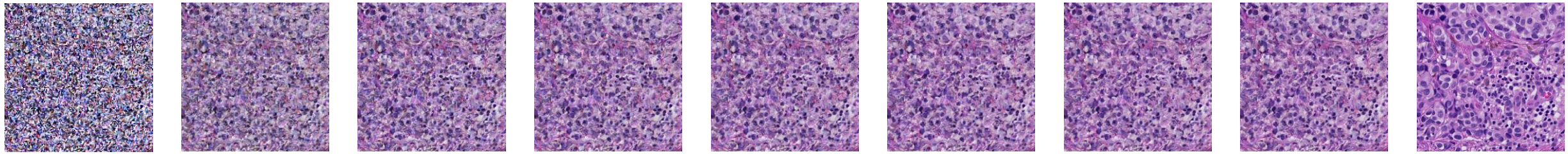

(a) Counter-diffusion process at the cell level

(b) Counter-diffusion process at the tissue level

Advantages of Laplace Distribution

■ Why laplace distribution is suitable for segmentation

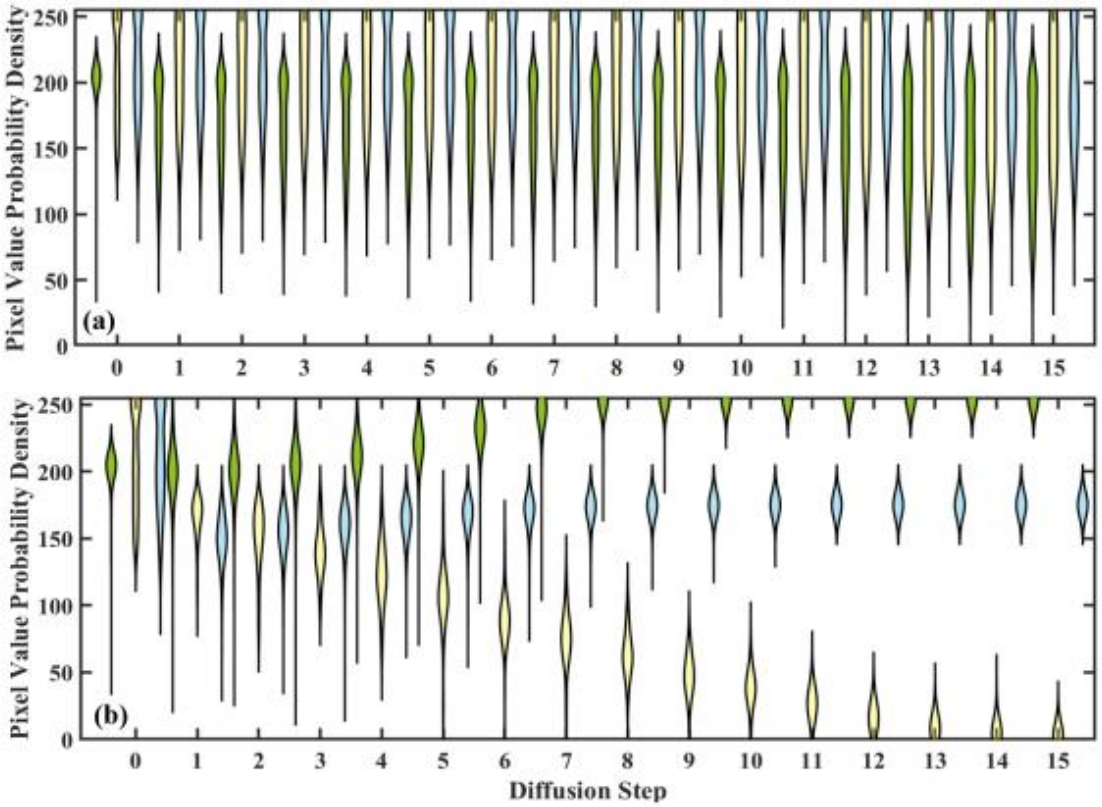

Figure 1. A comparative analysis of latent feature distributions between standard diffusion (a) and L-Diffusion (b). The latent feature distributions for individual components across various diffusion steps are denoted by violin plots in green, yellow, and cyan color.

- The sharpness of the Laplace prior promotes clearer **inter-class separation** in pixel-wise prediction tasks.

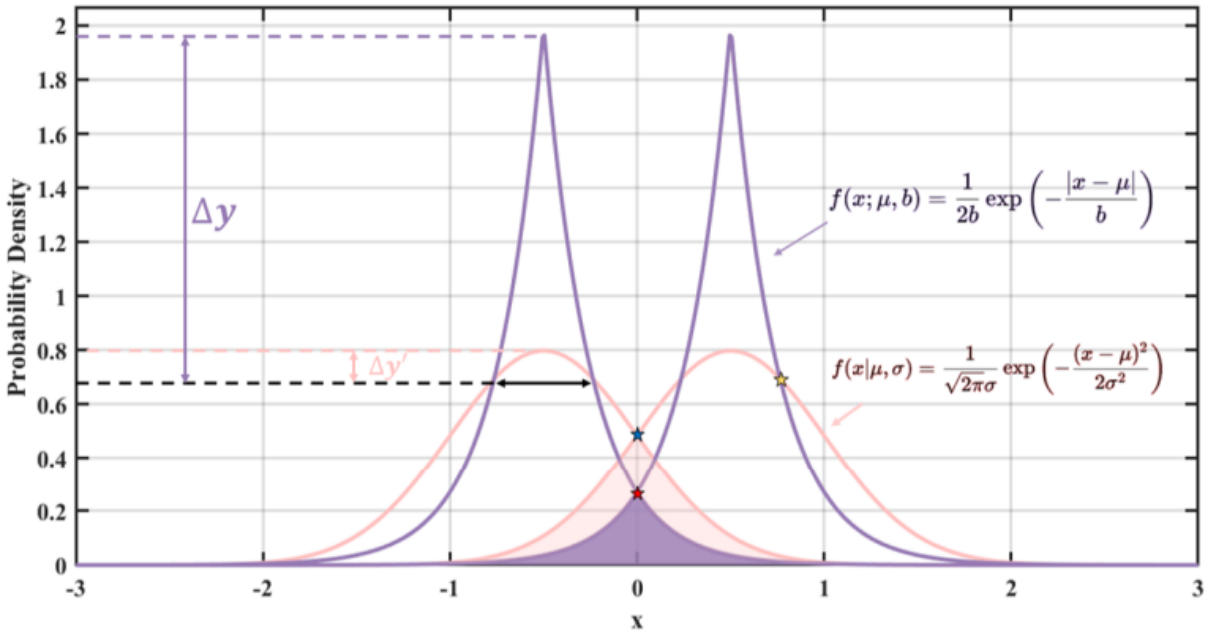

Figure 2. Illustration of Laplace and Gaussian distributions. The purple curve represents the Laplace distribution with means of −1 and 1, respectively, and a scale parameter of 0.25, while the pink curve depicts the Gaussian distribution with means of −1 and 1 and a variance of 0.5.

Derivation of Laplace Diffusion

■ How to get distribution from counter-diffusion

$$q(\tilde{x}_{t-1}|x_t) = \frac{q(x_t|\tilde{x}_{t-1}) \cdot q(\tilde{x}_{t-1})}{q(x_t)} \quad \text{.....} \quad (1)$$

$$q(\tilde{x}_{t-1}|x_t, x_0) = \frac{q(x_t|\tilde{x}_{t-1}, x_0) \cdot q(\tilde{x}_{t-1}|x_0)}{q(x_t|x_0)} \quad \text{.....} \quad (2)$$

$$q(\tilde{x}_{t-1}|x_t, x_0) = \frac{q(x_t|\tilde{x}_{t-1}, x_0) \cdot q(\tilde{x}_{t-1}|x_0)}{q(x_t|x_0)},$$

$$\Rightarrow -\sum_{n=1}^{N}\left(\frac{|x_t - \sqrt{\alpha_{(n,t)}}\tilde{x}_{t-1}|}{\sqrt{\beta_{(n,t)}}} + \frac{|\tilde{x}_{t-1} - \sqrt{\bar{\alpha}_{(n,t-1)}}x_0|}{\sqrt{1-\bar{\alpha}_{(n,t-1)}}} - \frac{|x_t - \sqrt{\bar{\alpha}_{(n,t)}}x_0|}{\sqrt{1-\bar{\alpha}_{(n,t)}}}\right). \quad (3)$$

$$q(\tilde{x}_{t-1}|x_t, x_0) \Rightarrow -\sum_{n=1}^{N}\left(\frac{|x_t - \sqrt{\alpha_{(n,t)}}\tilde{x}_{t-1}|}{\sqrt{\beta_{(n,t)}}} + \frac{|\tilde{x}_{t-1} - \sqrt{\bar{\alpha}_{(n,t-1)}}x_0|}{\sqrt{1-\bar{\alpha}_{(n,t-1)}}} - \frac{|x_t - \sqrt{\bar{\alpha}_{(n,t)}}x_0|}{\sqrt{1-\bar{\alpha}_{(n,t)}}}\right),$$

$$= -\sum_{n=1}^{N}\left(\frac{x_t - \sqrt{\alpha_{(n,t)}}\tilde{x}_{t-1}}{\sqrt{\beta_{(n,t)}}} + \frac{\tilde{x}_{t-1} - \sqrt{\bar{\alpha}_{(n,t-1)}}x_0}{\sqrt{1-\bar{\alpha}_{(n,t-1)}}} - \frac{x_t - \sqrt{\bar{\alpha}_{(n,t)}}x_0}{\sqrt{1-\bar{\alpha}_{(n,t)}}}\right),$$

$$= -\sum_{n=1}^{N}\left(\left(-\sqrt{\frac{\alpha_{(n,t)}}{\beta_{(n,t)}}} + \frac{1}{\sqrt{1-\alpha_{n,t-1}}}\right)\tilde{x}_{t-1} + C(x_t, x_0)\right). \quad (4)$$

$q(x_{t-1} \mid x_t)$ represents the probability distribution of the image at the previous moment when the noisy image at the current moment is known.

The **red box** refers to the scale parameter of the Laplace distribution, while the **blue box** refers to the mean value of the Laplace distribution. The data distribution for category n can be obtained after transformation

Impact of Different Modules

■ How to introduce supervised signals for Training

- Keep the error between the generated image and the original image low.

$$\mathcal{L}_{MSE} = \mathbb{E}_{x_0,\epsilon,t}\left[\|\epsilon - \epsilon_\theta(x_t, t)\|^2\right]$$

- Using contrastive learning, the same class is a positive sample, and different classes are negative samples.

$$\mathcal{L}_{CRT}^{k,k'} = -\log \frac{\text{Positive}(v_k^n, v_{k'}^n)}{\text{Positive}(v_k^n, v_{k'}^n) + \text{Negative}(v_k^n, v_i^{n'})}$$

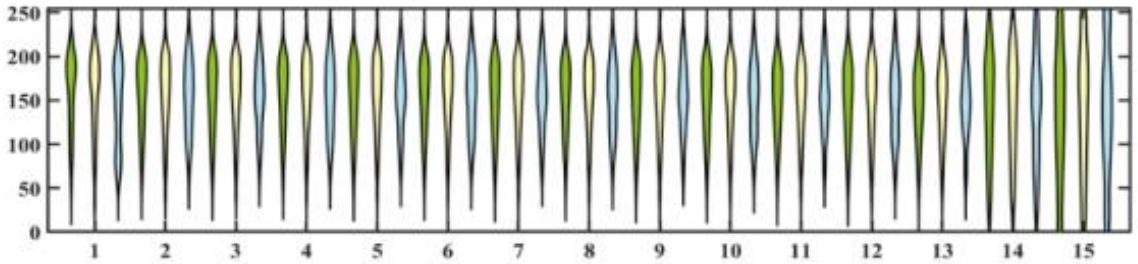

(a) Gaussian Distribution

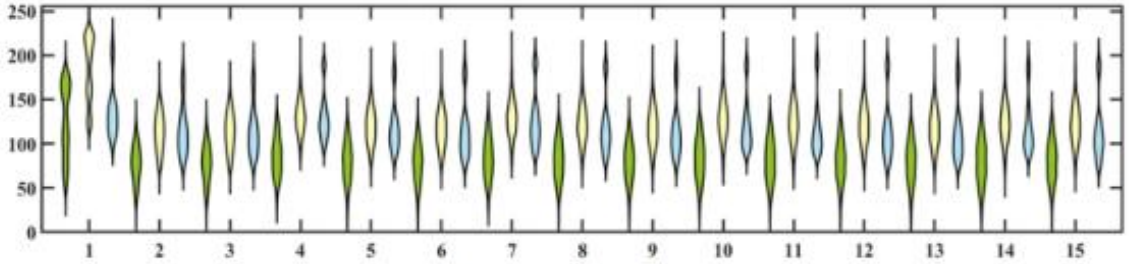

(c) Laplace Distribution

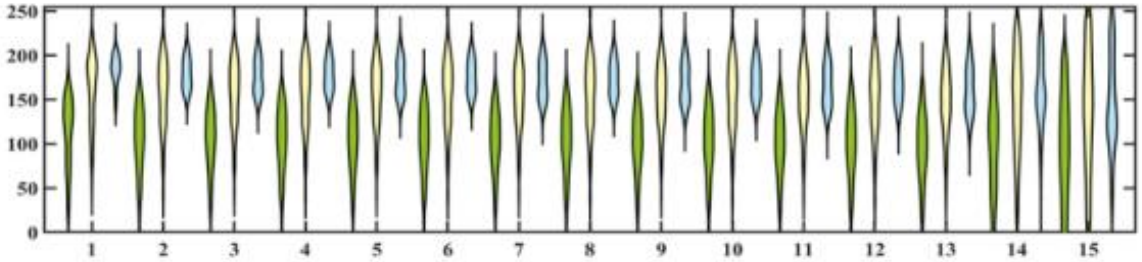

(b) Gaussian Distribution + Contrastive Learning

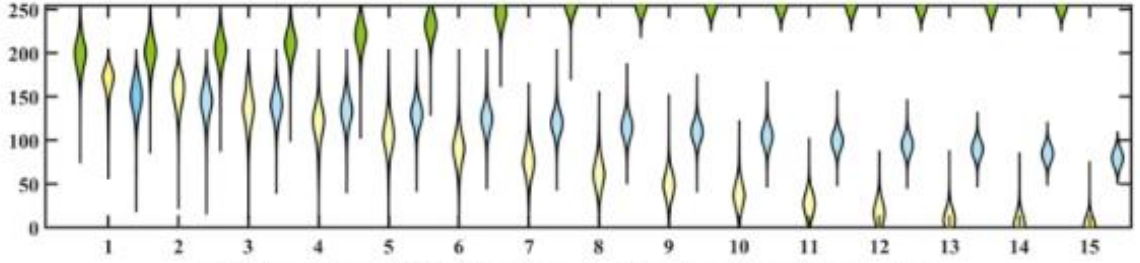

(d) Laplace Distribution + Contrastive Learning

Capabilities of L-Diffusion

■ Performance of L-Diffusion at the tissue and cell level

➢ L-Diffusion demonstrates strong performance in multi-category segmentation tasks

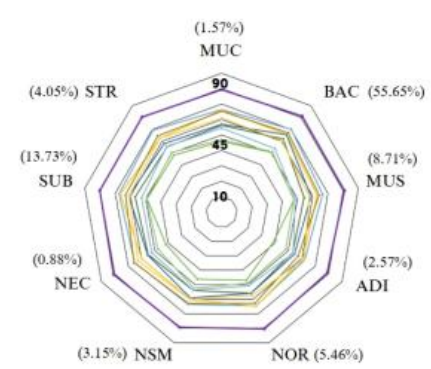

(a) CRCD-Tissue

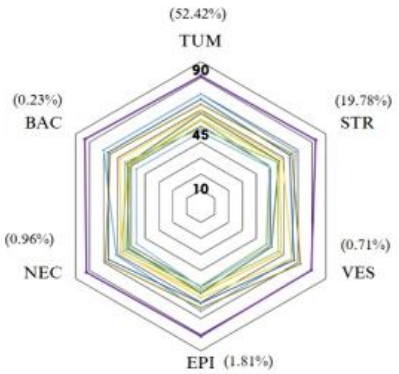

(b) PUMA-Tissue

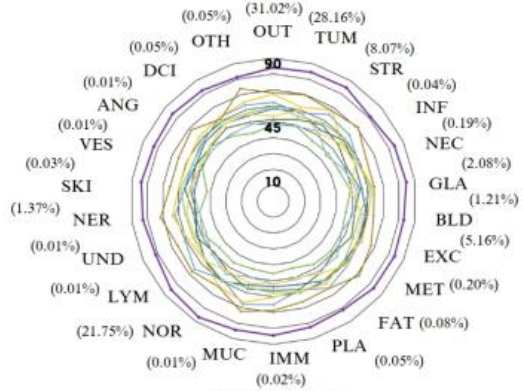

(c) BCSS-Tissue

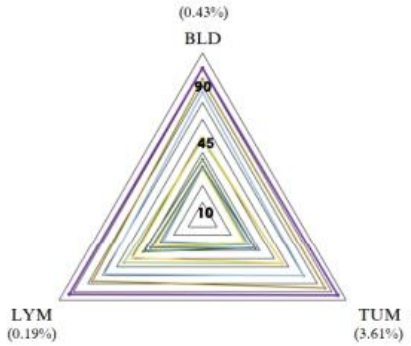

(d) CRCD-Cell

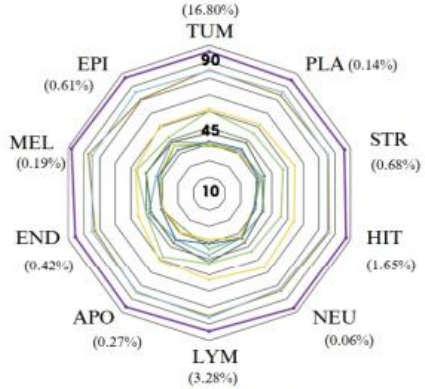

(e) PUMA-Cell

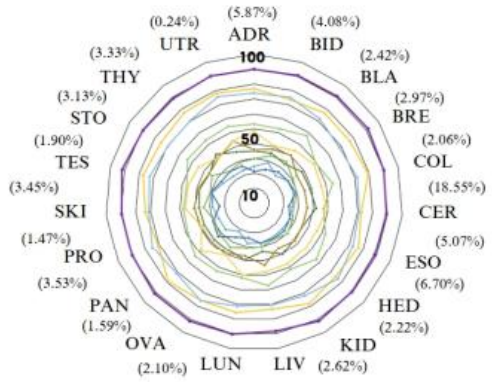

(f) PanNuke-Cell

FastFCN U-Net++ Swin-Unet SAMUS SAMed SAMPath DeepLabv3 DeepLabv3+ DenseASPP **L-Diffusion**

Table 1. Quantitative tissue segmentation performance (%) comparison. **Bold** and underling indicate the best and second-best performance.

Model	CRCD				PUMA				BCSS			
	DICE	MPA	mIoU	FwIoU	DICE	MPA	mIoU	FwIoU	DICE	MPA	mIoU	FwIoU
FastFCN	45.23	44.68	46.11	76.20	48.77	45.09	50.72	67.60	45.41	51.53	46.78	71.96
U-Net++	73.02	51.12	66.18	79.11	78.07	53.46	66.51	82.26	76.04	53.31	61.23	74.91
Swin-UNet	70.08	52.22	63.27	84.11	69.46	52.39	55.40	80.42	66.24	52.85	61.54	84.32
SAMUS	63.94	62.45	55.82	77.93	61.24	61.29	53.92	82.91	62.68	59.26	53.34	79.58
SAMed	70.63	50.38	58.38	78.08	62.56	57.39	64.48	70.74	67.51	51.71	56.48	75.79
SAMPath	77.54	66.70	63.65	86.28	84.95	57.79	66.30	83.92	78.10	62.83	67.44	87.12
UN-SAM	75.69	66.30	62.71	83.57	80.49	56.63	65.19	85.73	80.89	65.80	70.44	85.38
DeepLabv3	73.12	58.49	49.18	82.26	73.36	53.00	53.51	81.43	67.75	52.76	57.83	87.62
DeepLabv3+	77.04	58.14	52.80	81.88	80.85	58.41	48.01	88.55	86.31	56.53	50.19	84.30
DenseASPP	76.18	67.39	60.50	77.71	76.24	60.02	59.33	72.77	70.88	64.53	54.68	81.35
BoNuS	75.22	71.69	64.59	80.30	72.13	60.64	68.77	83.14	75.07	70.19	60.31	86.73
L-Diffusion	**82.38**	**80.19**	**80.17**	**86.47**	**92.11**	**88.03**	**81.62**	**91.77**	**89.24**	**82.33**	**83.49**	**91.17**
Improvement	*+4.84*	*+12.80*	*+16.52*	*+0.19*	*+7.16*	*+26.74*	*+15.11*	*+3.22*	*+2.93*	*+17.80*	*+16.05*	*+3.55*

Table 2. Quantitative evaluation of cellular segmentation performance (%). Metric calculations are only performed on foreground cells.

Model	CRCD				PUMA				PanNuke			
	DICE	MPA	mIoU	FwIoU	DICE	MPA	mIoU	FwIoU	DICE	MPA	mIoU	FwIoU
FastFCN	43.04	60.25	32.86	73.41	39.03	62.87	31.28	74.15	44.51	68.73	30.58	66.52
U-Net++	73.73	82.17	30.06	65.93	74.02	75.34	34.68	75.17	36.88	81.96	25.89	71.09
Swin-UNet	46.70	27.70	31.54	86.12	40.05	29.89	30.94	80.47	47.08	32.94	75.76	79.71
SAMUS	34.53	75.50	37.72	75.34	32.26	77.10	37.52	72.04	30.11	70.17	37.27	68.66
SAMed	70.85	61.21	34.93	69.66	66.88	64.57	31.93	73.02	72.60	61.33	26.59	67.95
SAMPath	79.02	87.97	82.03	81.23	81.62	80.79	74.50	80.68	72.33	82.79	38.08	80.46
UN-SAM	78.53	85.27	81.79	80.36	79.57	74.99	68.81	79.12	70.48	80.77	75.42	84.57
DeepLabv3	54.65	52.12	52.54	84.93	56.19	55.55	45.07	81.83	53.98	60.82	52.45	82.93
DeepLabv3+	63.43	59.01	71.66	79.38	65.99	55.92	75.00	82.59	71.46	55.17	72.41	87.30
DenseASPP	37.35	48.09	51.09	84.41	38.90	52.33	51.47	81.66	81.00	54.95	45.46	77.54
BoNuS	75.33	68.67	60.42	79.84	78.44	75.49	64.53	82.14	80.33	60.58	69.22	85.97
L-Diffusion	**96.11**	**94.94**	**92.62**	**95.34**	**88.57**	**90.38**	**86.19**	**83.13**	**94.78**	**93.46**	**90.18**	**92.18**
Improvement	*+20.09*	*+6.97*	*+10.59*	*+10.41*	*+6.95*	*+9.59*	*+11.19*	*+0.54*	*+13.78*	*+10.67*	*+14.42*	*+4.88*

ICML
International Conference
On Machine Learning

Thanks for watching!

Poster Time: Fri 18 Jul 7:30 a.m. CST — 10 a.m. CST

code

浙江大学
ZHEJIANG UNIVERSITY

VIPA